

# A Study on the Crystallization of Hydroxyapatite on Hydroxyethyl Cellulose Sponges

[1]Fathima Shahithaa, [2] Ang Pei Xinb, [3]Mohammed Al-Sibania,  
[4] Ab. Rahim, Mohd Hasbib, [5] Ahmed Al Harrasic, [6]Asiya Obaid Abdallah Al Saadia

The College of Arts and Sciences, Department of Biological Sciences and Chemistry, University of Nizwa Initial Campus, Birkat Al Mouz, P.O. Box 33, PC 616, Nizwa, Sultanate of Oman, bFaculty of Industrial Sciences & Technology, Universiti Malaysia Pahang, Lebuhraya Tun, Razak, 26300 Gambang, Kuantan, Pahang, Malaysia, bNatural and Medical Sciences Research Center, University of Nizwa Initial Campus, Birkat Al Mouz, P.O. Box 33, PC 616, Nizwa, Sultanate of Oman.

**Abstract:-** In this research, highly porous hydroxyethyl cellulose (HEC) sponges with different concentrations were prepared and cross linked by which the HEC sponges were changed from soluble into insoluble from in water which also enhanced its biodegradability. After the cross-linking process, hydroxyapatite (HA) crystals were formed on the HEC sponges through the crystallization process by using 20X simulated body fluid solution (SBF) solution, and the product was characterized by using FTIR, optical microscopy, FESEM with EDX, and XRD. From the FTIR results obtained, the presence of acetal group at the wavenumbers around 1022.20-1025.83 cm<sup>-1</sup> had showed the cross-linking process was succeeded. FTIR results after the crystallization showed peak of PO<sub>4</sub><sup>3-</sup> and CO<sub>3</sub><sup>2-</sup> which indicate the presence of HA crystals. This result was confirmed by using XRD and FESEM-EDX. There were extra peaks shown in the sample after crystallization compared to the sample before crystallization for the XRD analysis. This can proved the existence of the HA crystals. Further confirmation was done by using FESEM-EDX, and the element composition of HA crystals was revealed, which consisted of C, O, P and Ca. The morphology and the size of the HA crystals was determined by using FESEM. From the results obtained, it showed that HA crystals synthesized were in round shape, and the size of the HA crystals increased when the concentration of the HEC sponges increased. This is due to the polar hydroxyl side groups of the HEC molecules tend to interact with Ca<sup>2+</sup> during the HA crystallization process. The hydroxyapatite coated HEC sponges were highly stable in water and can be a promising scaffold material.

**Keywords:-** Hydroxyethyl cellulose, biomaterial, hydroxyapatite, freeze drying, simulated body fluid

## I. INTRODUCTION

Nowadays, intense research is being carried out to develop scaffolds for tissue engineering in an environmentally friendly way by green chemistry approach. According to Burg et al. (2000), the development of bone tissue engineering as an alternative has brought some advantages compared to the traditional ways of bone replacement such as allografts and autografts, vascularised grafts of the fibula or iliac crest and

other bone transport methods. These are some of the common standard treatments, but they are having some inherent limitation as well. For instance, the defect size and viability of the host bed will affect the bone grafting as it is avascular and dependent on diffusion. Besides, it may be problematic especially in large defects as the body may reabsorb the grafts before the osteogenesis is completed. For vascularized bone transplant, highly specialized technical expertise is needed for this sophisticated operation, the operating time needs to be prolonged, and the bone transplanted may be not large enough to match the big defect of the bone for immediate biomechanical stability (Philips and Nather, 2001). Furthermore, the donor tissue for autografts is always scarce, and significant morbidity of the donor site which usually associated with infection, hematoma and pain may be occurred.

Hence, bone tissue engineering is developed and applied as an alternative way for the traditional bone replacement method (Choong et al., 2011). The highly porous scaffold biomaterial is mainly used in the tissue engineering. Biomaterial can be defined as implanted materials which can replace or treat any tissues, organ or function of our body (Hollinger, 2012). It is used as a temporary matrix for the growth of bone which offers a specific environment and structure for tissue development. Tissue engineering has utilized the growth factors, scaffolds and mesenchymal stem cells for the bone regeneration process. Bone scaffolds produced with various compositions and structures has been developed successfully by scientists in different methods (Matassi et al., 2011). The scaffold will combine with the body cell to help in regenerating the damaged tissues (O'Brien, 2011).

Hydroxyapatite (HA) with the chemical formula of Ca<sub>10</sub>(PO<sub>4</sub>)<sub>6</sub>(OH)<sub>2</sub> is acted as the most significant biomineral and inorganic component in the bone tissue of the vertebrates (Chen et al., 2012). The high resemblance of HA with the inorganic component of bone matrix has encouraged the researchers to study on the synthetic HA. HA has high biocompatibility with the soft tissues like gums, muscle and skin. This characteristic makes it to be a suitable material for the orthopedic and dental implants compared to traditional allografts and metallic implants. Synthetic HA has been applied widely in the repairment and augmentation of bone,

other than as the implant's coating and fillers in bone or teeth (Zhou and Lee, 2011).

Bones and teeth are basically made up of HA and collagen fibers, which are organic/inorganic composites. Therefore, in bone tissue engineering, HA/polymer composites are applied extensively as they are chemically similar to the natural bone. The interaction and bonding between inorganic and organic phases have to be strong in order to possess a good mechanical property. In the living organisms, the bone cell and tissues starting from nano-blocks can combine to form self-assembled biomaterials under a controlled organic matrix. Therefore, in the process of synthesizing the synthetic HA, a matrix mediated mineralization is very important as it can mimic the structure of the natural bone and the environment of the growth of natural bone tissues (Li et al., 2010). Organic matrix can help in controlling the HA formation include the nucleation and crystal growth as well as the morphology of HA (Sinha et al., 2009).

HEC is a type of non-ionic polymer which is soluble in water. In order to strengthen the mechanical properties, the structure of HEC sponges is modified by cross-linking to remove the water soluble characteristics. There are numerous *in vitro* studies had been done on the affection and biocompatibility of the HA within the synthetic polymers like HEC on the biological function of bone-associated cells, and positive results had been obtained. These proved that the mineralization of HA on the polymeric substrates like HEC will aid in bone matrix synthesis (Chalal et al., 2014). The simulated body fluid (SBF) is often used for the formation of HA on biomaterial. SBF is an electrolyte solution which mimics the human blood plasma, as it has the inorganic composition that similar to the human blood plasma. In this study, HA crystal was formed by using the 20x SBF which has 20 times calcium and phosphate concentration compared to the conventional SBF.

The formation of the HA on the HEC sponges by using the SBF solution is related to the theory of crystallization. There are two steps involved in the crystallization process, which are nucleation and crystal growth. The porous structures of the HEC sponges provide numerous pores for the growth of HA crystals on it. When this product is applied for the *in vitro* or *in vivo* tests, the porous structure of HEC sponges and HA will permit the flow of extra cellular fluid through the inner structure of this biomaterial. Consequently, high osteoconductivity, mechanical interlocking for firm fixation of material will be created. Other than these, the adhesion between the natural and synthetic bone tissue will be enhanced through the formation of the apatite layer (Chavan et al., 2010). Hence, this will be an excellent and potential biomaterial for the bone tissue engineering.

In this research, hydroxyapatite is formed through the process of crystallization on the hydroxyethyl cellulose (HEC) sponges of varying concentrations.

## II. EXPERIMENTAL SECTION

### A. Materials

Hydroxyethyl cellulose (HEC) was purchased from Nacalai Tesque, Japan. Glutaraldehyde, grade II, 25% in H<sub>2</sub>O was purchased from Sigma-Aldrich, USA. Phosphoric acid was purchased from R&M Chemical, UK. Analytical reagent grade acetone was purchased from Bendosen. Among the chemicals used for preparing the SBF solution, sodium chloride (NaCl) was purchased from Merck KGaA, Germany, calcium chloride dehydrate, (CaCl<sub>2</sub>.2H<sub>2</sub>O) was purchased from Fisher Chemical, UK, sodium bicarbonate (NaHCO<sub>3</sub>), potassium chloride (KCl), magnesium chloride hexahydrate (MgCl<sub>2</sub>.6H<sub>2</sub>O) and sodium dihydrogen phosphate (NaH<sub>2</sub>PO<sub>4</sub>.H<sub>2</sub>O) were purchased from Sigma-Aldrich, USA. Deionized water was used throughout the research for preparing all the solutions and cleaning the glassware.

### B. Experimental

#### ➤ Preparation of the Hydroxyethyl Cellulose Solution

Prior to the experiment, all the glassware were washed and cleaned with soap and deionized water to prevent contamination of the sample. The HEC solution with five different concentrations: 1 wt%, 3 wt%, 5 wt%, 7 wt% and 10 wt% were prepared by dissolving 1 g, 3 g, 5 g, 7 g and 10 g HEC powder with 100 mL of deionized water in five separated beakers. Deionized water was used as the solvent it has no charge, therefore it will not react with the HEC powders. The solutions in the beakers were then left to stir overnight by using magnetic stirrers in order to obtain homogeneous solutions.

#### ➤ Preparation of the Hydroxyethyl Cellulose Sponges

After the homogeneous HEC solutions (1 wt%, 3 wt%, 5 wt%, 7wt% and 10 wt%) were obtained, the HEC sponges were prepared through the freeze drying process. Freeze drying is a process of removing frozen solvents from a material through sublimation and desorption. Before the samples were placed into the freeze dryer, the five beakers contained with HEC solution were put into a freezer with the temperature of -80°C for five days until the samples were completely turned into solid form. In fact, one day of freezing is enough for the sample to turn solid, but the longer the time of freezing, the better the condition for the next step. The samples should to be completely frozen before placing under vacuum in the freeze dryer, to prevent the unfrozen part expands outside of the container. The beakers were placed slanting on the wall inside the freezer, in order to increase the surface area of the sample which can help in the freeze dry process later on. After five days, the samples were taken out from the freezer and put into the freeze dryer for four days to remove the water contained in the samples. HEC sponges were then formed.

#### ➤ Cross-linking of Hydroxyethyl Cellulose Sponges

The purpose of carry out the cross-linking process is to remove the water solution characteristic of the HEC sponges. The HEC sponges should have good integrity in the aqueous solution so that it is practicable in tissue engineering. Cross-linking process was carried out by using the glutaraldehyde

which acted as the cross-linking agent, acetone and phosphoric acid which is the acid catalyst in the reaction. Firstly, HEC sponges in five different concentrations were cut into small pieces and put into five different petri dishes. Then, 500  $\mu$ L glutaraldehyde, 3mL acetone and 5-8 drops of phosphoric acid were added into each petri dish with the help of micropipette and pipette. All the HEC sponges must be completely immersed in the chemical solution. Otherwise, the amount of glutaraldehyde, acetone and phosphoric acid must be increased by two times. The petri dishes containing the HEC sponges with the cross-linking chemicals were then left for 24 hours at room temperature. After 24 hours, the cross-linking reaction was stop by rinsing the HEC sponges with the deionized water. The solubility of the HEC sponge was checked by immersing it in the beaker containing deionized water.

➤ *Preparation of 20× Simulated Body Fluid Solution for Crystallization of Hydroxyapatite on Hydroxyethyl Cellulose Sponges*

20× SBF solution was used to form the HA crystal on the HEC sponges in this reasearch. The SBF solution was prepared based on Tas and Bhaduri (2004) and Mavis et al. (2009). There are several chemical needed to prepare the SBF solution, including sodium chloride, potassium chloride, calcium chloride dehydrate, magnesium chloride hexahydrate, sodium dihydrogen phosphate and sodium bicarbonate. The amount needed is listed in the Table 3.1 below. In order to prepare 500 mL of 20× SBF solution, the first five chemicals listed in the table was measured and dissolved in 400 mL deionized water. The solution was stirred continuously using a glass rod until all the chemical was dissolved completely in the deionized water. Then, the volume of the stock solution was topped up to 500 mL and stored at room temperature in a capped glass bottle.

Table 1: Reagents for preparing 500 mL of 20× SBF solution

Order	Reagent	Amount (g)	Molarity (mM)
1	NaCl	58.443	2000
2	KCl	0.373	10
3	CaCl <sub>2</sub> .2H <sub>2</sub> O	3.675	50
4	MgCl <sub>2</sub> .6H <sub>2</sub> O	1.016	10
5	NaH <sub>2</sub> PO <sub>4</sub> .H <sub>2</sub> O	0.250	7.24
6	NaHCO <sub>3</sub>	0.840	20

Source: Chalal et al. (2013)

SBF is supersaturated with respect to apatite. Therefore, any small mistake that happened during the preparation of SBF may lead to the formation of apatite precipitate in the solution. SBF solution should be colourless and transparent. When there is precipitate observed in the solution, the SBF solution preparation is considered as fail and should be discarded and restart with clean glassware (Kokubo and Takadama, 2006).

➤ *Crystallization of Hydroxyapatite on Hydroxyethyl Cellulose Sponges*

The SBF solution prepared previously was used for the crystallisation of hydroxyapatite. Before the scaffold mineralization, 100 mL of the stock SBF solution was transferred into a beaker. After that, 0.168 g of NaHCO<sub>3</sub> was added to increase the pH value to pH 6.5 (Tas and Bhaduri, 2004) and dissolved completely. The HEC sponges with the concentration of 1 wt%, 3 wt%, 5 wt%, 7wt% and 10 wt% in small pieces which had cross linked previously were put in the tissue culture testplate. Then 3 mL of SBF solution was pipetted and added into each hole which contained 1 piece of HEC sponges. The samples must be fully immersed in the SBF solution. The tissue culture testplate was then covered with aluminium foil to prevent contamination of samples and left for 48 hours at room temperature. After 48 hours, the samples were rinsed with deionized water to remove the salt residue and left to dry in room temperature before proceeding to the characterization.

In fact, there are two precaution steps that should be followed during the preparation of SBF solution. Firstly, plastic container should be used instead of glass container and make sure that there is no scratch on the surface of plastic container. This is due to apatite nucleation may be induced at the surface of a container or the edges of scratches. Secondly, the reagents used should not be dissolved at the same time. One reagent should be dissolved completely before proceeding with the next reagents (Kokubo and Takadama, 2006).

C. *Characterization of hydroxyapatite on hydroxyethyl cellulose*

➤ *Fourier Transform Infrared (FTIR) Spectroscopy*

Fourier Transform Infrared (FTIR) spectroscopy was used to determine the functional group presented in the samples before cross-linking, after cross-linking and after crystallization. Attenuated Total Reflection (ATR) technique was used in this research. This was done by using Perkin Elmer spectrum 100 spectrophotometer in the range of 700 cm<sup>-1</sup> to 4000 cm<sup>-1</sup>, with resolution of 4 cm<sup>-1</sup> and 10 scans per sample. The crystal area was cleaned and background was collected before the analysis. Then, small pieces of HEC sample before cross-linking, after cross-linking and after crystallization were placed directly onto the small crystal area to determine the FTIR spectrum.

➤ *Field Emission Scanning Electron Microscopy (FESEM)*

JEOL Field Emission Scanning Electron Microscopy (FESEM) was used to determine the morphology and size of the HEC pores and HA crystal formed on the HEC sponges. It is operated under vacuum condition. Before the sample analysis, sample preparation was done by coating a thin layer of platinum on the sample which was in a very dry condition. This is due to HEC sponges is a non-conductive material and it was done by using a sputter coater in order to provide a current conductive surface on the sample. Besides, FESEM was worked with Energy Dispersive X-Ray (EDX) to determine the elemental composition of HA crystal on the HEC sponges. Ca/P ration was determined by using EDX as

well.

#### ➤ Optical Microscopy

Optical microscopy was performed to observe the surface morphology of the HEC sponges and the HA crystal formed on the HEC sponges. Highest resolution of Nikon E100 microscope  $1280 \times 960$  was used in this analysis, and it provided the magnification to 4, 10, 40 or 100 times. This type of microscope operates by using the visible light and a system of lenses to magnify the image of the small sample. Besides, Dino Eyes Software was installed and used in the computer that connected to the microscope, in order to capture the image of the HEC sponges and HA crystals on it. The sample was put on the microscope glass slide and placed on the stage. Then the light intensity and the magnification of the lenses were adjusted to obtain the best image of morphology of samples. Since the optical microscopy is performed by the light passing through the sample, the sample have to be as thin as possible in order to obtain a better result.

#### ➤ X-Ray Diffraction (XRD)

X-Ray Diffraction (XRD) was conducted to determine the presence of HA crystal on the HEC sponges. Rigaku Miniflex II Diffractometer was used in this analysis with  $\text{CuK}\alpha$  (wavelength = 1.54 Å) as the x-ray source. It was generated at 30 kV and 15 mA in  $2\theta$  range of  $3^\circ$  to  $60^\circ$ , with the scan rate of 1 degree per minute. 1 cm  $\times$  1 cm HEC sponges before crystallization and after crystallization of HA were used for the

### III. RESULTS AND DISCUSSION

#### A. HEC SPONGES

During the preparation of 1 wt%, 3 wt%, 5 wt%, 7 wt% and 10 wt% of HEC solutions, homogeneous solutions were formed after the stirring, Figure 4.1. The viscosity and colour intensity of the HEC solutions increased when the concentration increased. This is due to there are more particles presented in the HEC solution of higher concentration.

HEC sponges were produced through the freeze drying process (Figure 4.2). The sizes of the HEC sponges formed were different according to the concentration of the HEC solution. The lower the concentration of the HEC solution, the smaller the size of the HEC sponges formed. This is because of there are more water contained in the HEC solution of low concentration, and more water molecules will be removed during the freeze drying process.

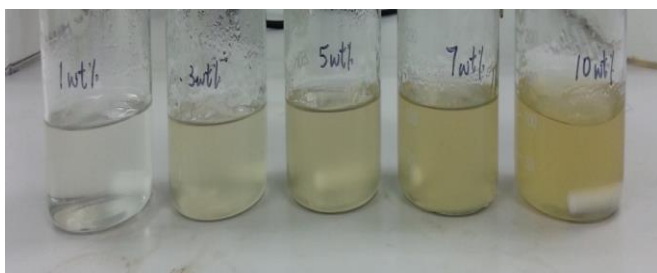


**Fig 4.1:** HEC solutions after stirring with concentration of 1 wt%, 3 wt%, 5 wt%, 7 wt% and 10 wt% from left to right

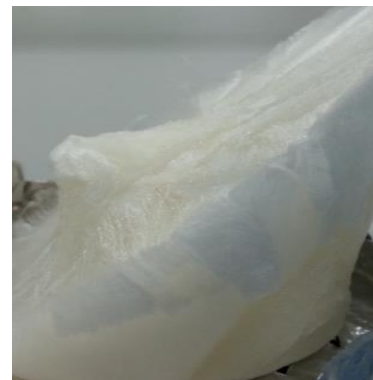


**Fig 4.2:** HEC sponges formed after freeze drying process

#### B. CROSS-LINKING OF HEC SPONGES

In order to fabricate a scaffold with good integrity for the application in tissue engineering, cross-linking process was done on the HEC sponges to remove the water-soluble property. After immersing the HEC sponges in the mixture of glutaraldehyde, acetone and phosphoric acid with a fixed amount for 24 hours (Figure 4.3), the HEC sponges were washed by deionized water and the water solubility of HEC sponges was tested by immersing in the deionized water. The result showed that HEC sponges after cross-linking was not soluble in deionized water (Figure 4.4). This proves that the water-soluble ability of the HEC was successfully removed through the cross-linking process. The removal of the water-soluble ability of the HEC is very important to ensure that it will not dissolve in the SBF solution during the incubation.



**Fig 4.3:** HEC sponges immersed in cross-linking agents



**Fig 4.4:** HEC sponges insoluble in water after cross-linking

**C. CRYSTALLIZATION OF HYDROXYAPATITE ON HEC SPONGES**

The formation of HA crystal was done on the HEC sponges which had been cross-linked previously. Five different concentrations of HEC sponges of in pieces which had been cross-linked were immersed into the 20× SBF solution in cell culture plate for 48 hours as shown in figure 4.5. Nominal ion concentrations of SBF compare with human blood plasma is given in table 2. The SBF solution that prepared was a clear solution without any precipitation. After 48 hours, some white precipitate can be seen in the solution and the surface of HEC sponges as shown in figure 4.6. This “precipitate” is actually the white HA crystals which formed in the SBF solution. The HEC sponges were then remove from the SBF solution and the salt residue was rinsed off with deionized water. The sample was then left to dry under normal room temperature in the desiccators before the characterization part.

**Table 2.** Nominal ion concentrations of SBF compare with human blood plasma

Ion	Ion concentration(mM)	
	Blood Plasma	SBF
Na <sup>+</sup>	142.0	142.0
K <sup>+</sup>	5.0	5.0
Mg <sup>2+</sup>	1.5	1.5
Ca <sup>2+</sup>	2.5	2.5
Cl <sup>-</sup>	103.0	147.8
HCO <sub>3</sub> <sup>-</sup>	27.0	4.2
HPO <sub>4</sub> <sup>2-</sup>	1.0	1.0
SO <sub>4</sub> <sup>2-</sup>	0.5	0.5
pH	7.2-7.4	7.40



**Fig 4.5:** Immersion of HEC sponges in 20× SBF solution (beginning)

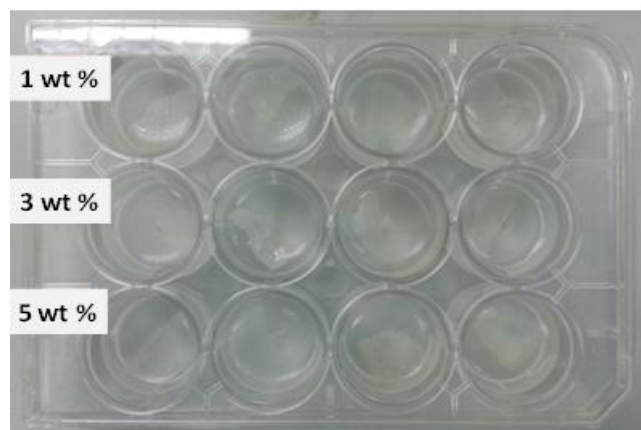


**Fig 4.6:** Immersion of HEC sponges in 20× SBF solution (after 48 hours)

**D. Fourier Transform Infrared (FTIR) Spectroscopy Study**

ATR-FTIR was used to determine the functional groups that presented in the HEC sponges. Figure 4.7 shows FTIR spectra of the combination (1 wt%, 3 wt%, 5wt%, 7 wt% and 10 wt%) of HEC sponges before the cross-linking. From the result obtained, there is no much difference of the spectrum between the 1 wt%, 3 wt%, 5wt%, 7 wt% and 10 wt% of HEC sponges. The broad peaks with the wavenumbers 3380.57 cm<sup>-1</sup> to 3384.79 cm<sup>-1</sup> indicate the -OH stretching vibration. Due to the presence of hydroxyl group, HEC sponges are soluble in water. Therefore, cross-linking was carried out to remove the hydroxyl group. The peaks at 2880.02-2881.62 cm<sup>-1</sup> represent the C-H stretching vibration. The peaks around 1642.84-1649.05 cm<sup>-1</sup> are corresponding to the bending mode of the water absorbed naturally (Azzaoui, 2015). Peaks appeared at 1354.80-1356.54 cm<sup>-1</sup> represent the C-H vibration. The sharp peaks at 1052.94-1054.02 cm<sup>-1</sup> indicate the C-O-C stretching vibration in ether group or C-O stretch in primary alcohol. The small peaks at wavenumbers around 885.20-886.01 cm<sup>-1</sup> represent the C-C stretching vibration.

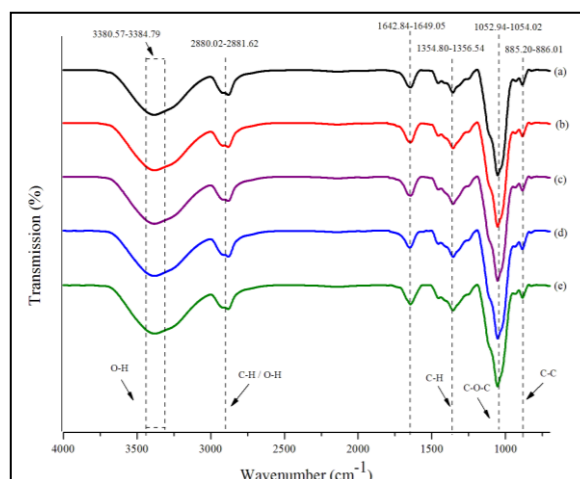


**Fig 4.7:** Combined FTIR spectra of (a) 1 wt% (b) 3 wt% (c) 5 wt% (d) 7 wt% (e) 10 wt% HEC sponges before cross-linking

The combined FTIR spectra of different concentrations of HEC sponges after cross-linking are shown in figure 4.8. There is no much difference of the spectrum between the 1 wt%, 3 wt%, 5wt%, 7 wt% and 10 wt% of HEC sponges after cross-linked. From the spectrum obtained, the broad peaks with the wavenumbers 3369.12 cm<sup>-1</sup> to 3390.66 cm<sup>-1</sup> indicate the -OH stretching vibration. It is lower compared to the -OH spectrum of the sample before cross-linking. This shows that the water soluble characteristic has been reduced after cross-linked with glutaraldehyde. The peaks at 2881.80-2925.96 cm<sup>-1</sup> represent the C-H stretching vibration. The peaks around 1644.52-1649.86 cm<sup>-1</sup> are corresponding to the bending mode of the water absorbed naturally (Azzaoui, 2015). The presence of this peak may be due to the water molecule that still contained in the sample and not fully dried after washing with deionized water. The peaks around 1456.18-1458.51 cm<sup>-1</sup> indicate the CH<sub>2</sub> or CH<sub>3</sub> in aliphatic compounds are stronger compared to the samples before cross-linking. This is due to the formation of acetal group after the cross-linking. Peaks appeared at 1355.86-1358.31 cm<sup>-1</sup> represent the C-H vibration. The sharp peaks at 1053.90-1056.72 cm<sup>-1</sup> indicate the C-O-C stretching vibration in ether group or C-O stretch in primary alcohol. The presence of acetal group due to the reaction between HEC and glutaraldehyde has contributed to the peaks at the wavenumber around 1022.20-1025.83 cm<sup>-1</sup>. The small peaks at wavenumbers around 888.15-889.70 cm<sup>-1</sup> represent the C-C stretching vibration., (Azzaoui 2015) (Khairy M.Tohamy 2018).

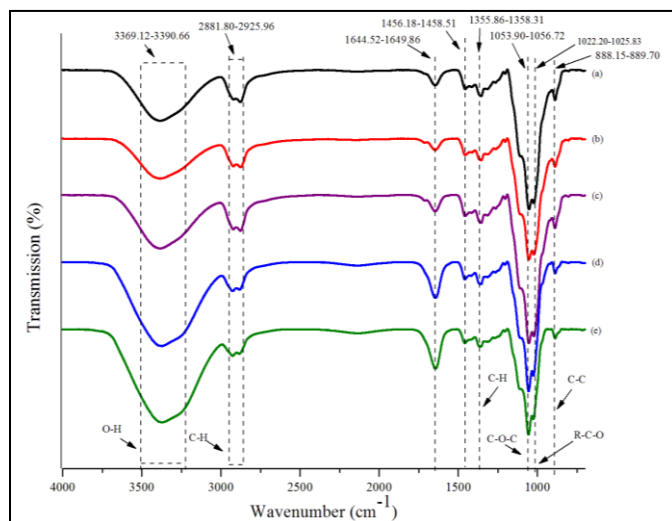


**Fig 4.8:** Combined FTIR spectra of (a) 1 wt% (b) 3 wt% (c) 5 wt% (d) 7 wt% (e) 10 wt% HEC sponges after cross-linking

Figure 4.9 shows the combined FTIR spectra of HEC sponges after crystallization of HA. From the spectra obtained, O-H stretching vibrations are shown in the broad peaks at the wavenumbers 3378.50-3379.68 cm<sup>-1</sup>. The peaks at 2881.44-2930.50 cm<sup>-1</sup> and 1355.35-1357.00 cm<sup>-1</sup> are attributed to the C-H stretching vibration. Besides, H<sub>2</sub>O band is observed at the peak with the wavenumbers around 1638.28-1642.62 cm<sup>-1</sup> which may be the water molecule associated with the HA particles. The peaks at 1050.46-1052.84 cm<sup>-1</sup> show the PO<sub>4</sub><sup>3-</sup>. These can prove the presence of HA on the HEC sponges. Other than these, CO<sub>3</sub><sup>2-</sup> can be observed at the weak band with the wavenumbers 1413.78-1421.04 cm<sup>-1</sup> and

872.01-889.67 cm<sup>-1</sup>. The carbonate ion indicates that it is B-type carbonate apatite (CO<sub>3</sub> substituting PO<sub>4</sub>) (Chalal et al., 2014). It may be caused by the absorption of CO<sub>2</sub> from the atmosphere to the HA particles.

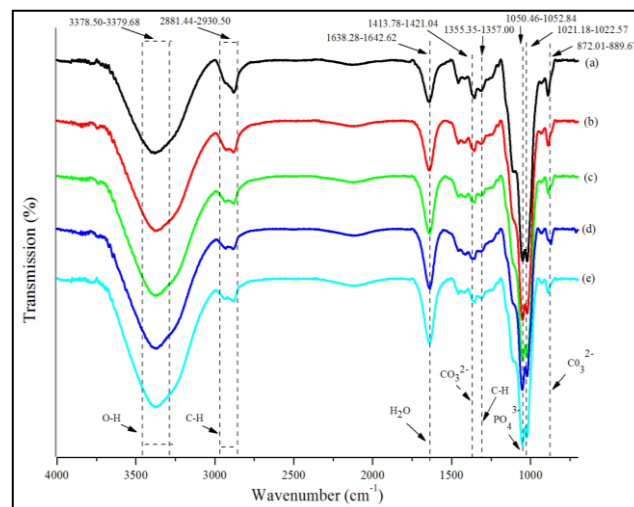


**Fig 4.9:** Combined FTIR spectra of (a) 1 wt% (b) 3 wt% (c) 5 wt% (d) 7 wt% (e) 10 wt% HEC sponges after crystallization of HA

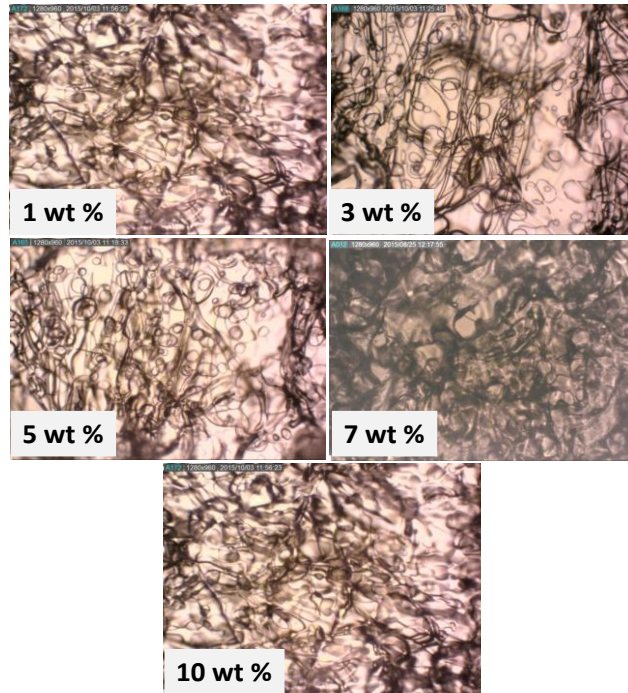
*E. Optical Microscopy*

Optical microscopy was done on the 5 different concentrations of HEC sponges before cross-linking, after cross-linking and after crystallization of HA. These were done by using 10X magnification. However, since the resolution of optical microscope is quite poor, characterization by using FESEM was done to observe the morphology of HA crystals as well.

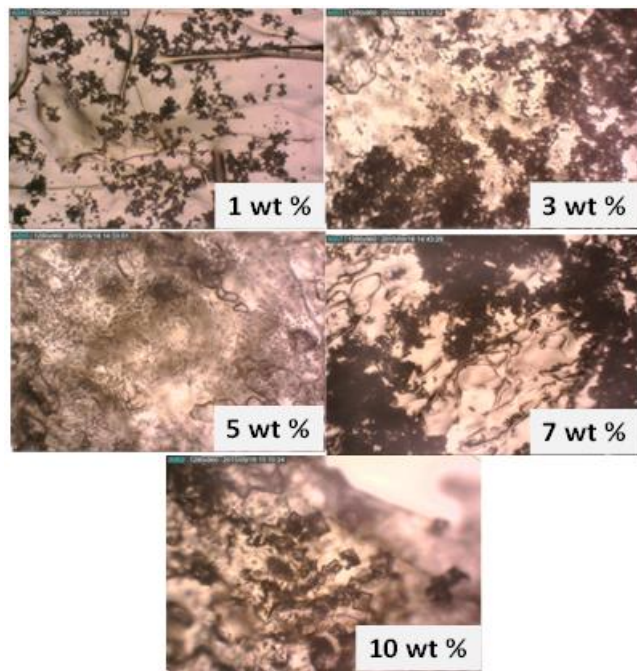
Figure 4.10 (a), (b), (c), (d) and (e) show the morphology of HEC sponges before the crystallization step. The pores of the HEC sponges can be clearly seen. However, there is a difficulty to measure the size of the pores with optical microscope. Therefore, the actual effect of the HEC concentration on the pore size cannot be determined. Theoretically, HEC sponges with higher concentration will have smaller pore size. This is due to the HEC sponges with higher concentration is more viscous and the pore wall tend to be thicker and more homogeneous. Therefore, the morphology of the sponge's surface will be denser (Ikeda et al., 2014). This is a vital factor to a successful scaffold in tissue engineering. The pore structures of the HEC sponges did not affected after the cross-linking step. The space in the pores was utilized for the cell growth as well as metabolic wastes and nutrients-exchange between the scaffold and the environment (Zulkifli et al., 2013).

Figure 4.11 (a), (b), (c), (d) and (e) reveal the optical microscopy images of the HEC sponges after coated with the HA crystals. HA crystals formation was done by immersing the cross-linked HEC sponges into the 20x SBF solution for 48 hours. It showed that the HA crystals formed on the HEC sponges with higher concentration is larger in size compared to the HA crystals formed on HEC sponges with lower concentration. However, the exact size and shape of the

crystals cannot be determined by using optical microscope due to its poor resolution and magnification. Therefore, further analysis was done by using the FESEM.



**Fig 4.10:** Optical microscopy image of (a) 1wt% (b) 3wt% (c) 5wt% and (e) 10 wt% HEC sponges before cross-linking



**Fig 4.11:** Optical microscopy image of HA crystallization on (a) 1 wt% (b) 3 wt%, (c) 5 wt% and (e) 10 wt% HEC sponges

**F. Field Emission Scanning Electron Microscopy (FESEM)**

FESEM was done to determine the morphology of the HA crystals. Figure 12 shows the FESEM images of HA crystals formed on 1 wt%, 3 wt%, 5 wt% and 10 wt% of HEC sponges respectively. From the images obtained, the pores of the HEC sponges cannot be seen clearly, and this may be due

to the surface of the HEC sponges has been covered by the HA crystals and the pores were blocked by the HA crystals. The results revealed that the HA crystals formed were in round shapes. The average size the HA crystals formed on 1 wt%, 3 wt%, 5 wt% and 10 wt% HEC sponges are around 0.10-0.13  $\mu\text{m}$ , 0.18-0.21  $\mu\text{m}$ , 0.19–0.23  $\mu\text{m}$  and 0.53–0.69  $\mu\text{m}$  respectively. The size of the HA crystals were increasing with the concentration of the HEC sponges.

Zhang et al. (2009) stated that the crystal growth in HEC is strongly depends on the interaction between the HEC molecules and the crystal surface. HEC with higher concentration may lead to the interaction between the HEC molecules and crystal surface sufficient to lower the crystal surface energy as well as to stabilize the crystals in metastable phase. The difference in concentration of HEC will affect the morphology and size of the crystals formed. When the HEC concentration increased, there is less space between the HEC molecules and become entangled or aggregated. This will alter the interaction between the HEC molecules and HA crystals. Polar hydroxyl side groups of the HEC molecules tend to interact with  $\text{Ca}^{2+}$  during the HA crystallization process, to create the nucleation sites. The interface energy is then reduced and eases the formation of metastable phase.

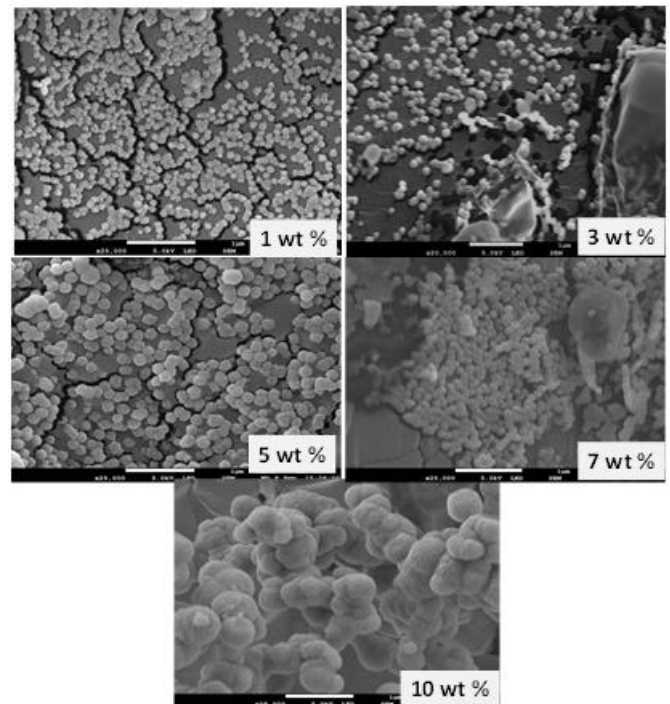


**Fig 4.12:** FESEM image of HA on 3 wt% HEC sponges after 48 hours incubation in 20× SBF solution

Other than these, EDX was performed to determine the mineral phase and elemental composition of HA crystals formed on the HEC sponges. Figure 4.13 shows the FESEM-EDX image of 10 wt% HEC sponges after the incubation in the 20× SBF solution for 48 hours. Table 3, reveals the element which consisted in the HA-coated HEC sponges and their respective weight percentage and atomic percentage. There are four main elements in the mineralized HEC sponges, which are carbon (C), oxygen (O), phosphorus (P) and calcium (Ca). C and O could be from the HEC while P and Ca could be from

the mineral phase. The percentage of C and O are higher than Ca and P may be due to the area selected for the EDX analysis is not fully covered with the HA crystals. From the EDX data, Ca/P ratio was calculated and 1.37 was obtained. This result is comparable with the study done by Cengiz et al. (2008) which showed the Ca/P ratio of 1.34 after the HA crystallization process by using SBF solution. Normal human bone has a Ca/P ratio of 1.67.

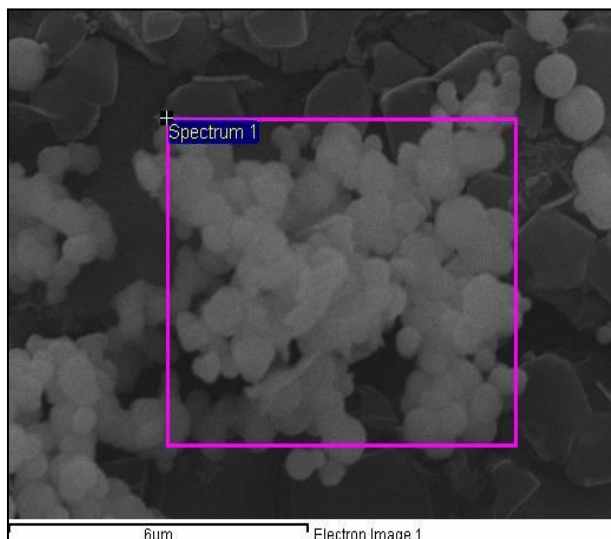


**Fig 4.13:** FESEM-EDX image of 10 wt% HEC sponges after 48 hours incubation in 20x SBF solution

**Table 3:** Composition of elements of HA crystals on HEC sponges

Element	Weight %	Atomic %
Carbon, C	27.42	36.76
Oxygen, O	55.13	55.48
Phosphorus, P	6.28	3.27
Calcium, Ca	11.16	4.48
Totals	100	100

**G. X-Ray Diffraction (XRD)**

XRD analysis was done to determine the presence of the HA crystals on the HEC sponges. Figure 4.14, show the x-ray diffractograms of combined, 1 wt%, 3 wt%, 5 wt%, 7 wt% and 10 wt% HEC sponges. It can be clearly seen that there is not much differences between these 5 x-ray diffractogram. From the results obtained, most of them show amorphous hump at 14.67 °, 15.03 °, 14.29 ° and 14.66 ° for 1 wt%, 3 wt%, 7 wt% and 10 wt% HEC sponges. Other than these, there are two sharp peaks at 21.42 ° and 23.75 ° for 1 wt% HEC sponges, 20.34 ° and 21.49 ° for 3 wt% HEC sponges, 21.44 ° and 23.74 ° for 5 wt% HEC sponges, 21.24 ° and 23.56 ° for 7 wt% HEC sponges, 21.38 ° and 23.67 ° for 10 wt% HEC sponges.

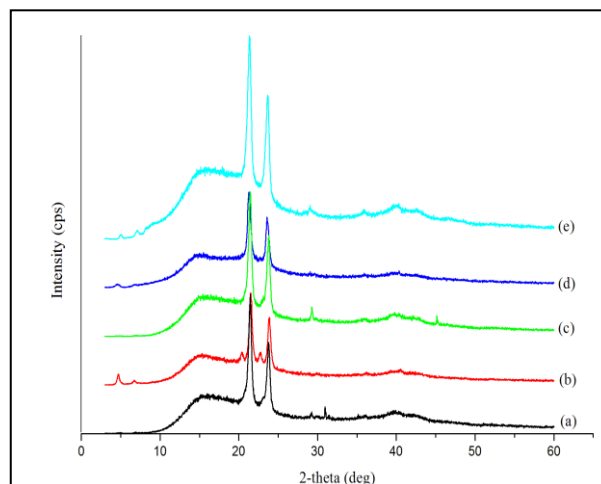


**Fig 4.14:** Combined XRD pattern of (a) 1 wt% (b) 3 wt% (c) 5 wt% (d) 7 wt% (e) 10 wt% HEC sponges before crystallization

From the results obtained, the amorphous hump and the first two peaks are same as the x-ray pattern shown in pure HEC sponges. Other than these, there are extra peaks compared to pure HEC sponges, which appeared at 29.42 °, 47.58 ° and 48.65 ° (hydroxyapatite) for the HA crystals on 1 wt% HEC. However, the intensity of the peaks are quite low, and this may be due to the HA crystals formation are not fully on the surface of the sample but inside the pores of HEC sponges. The extra peaks were shown at 29.11 ° (hydroxyapatite, 210), 31.74 ° (hydroxyapatite, 211) and 31.97 ° (hydroxyapatite, 000) for HA crystals on 3 wt% HEC sponges, 32.12 ° (hydroxyapatite), 45.84 ° (hydroxyapatite, 211) and 56.85 ° (hydroxyapatite, 313) for HA crystals on 5 wt% HEC sponges, 29.20 ° (hydroxyapatite, 120), 31.91 ° (hydroxyapatite, 000), 45.64 ° (hydroxyapatite, 203) and 56.64 ° (hydroxyapatite, 114) for HA crystals on 7 wt% HEC sponges, 31.86 ° (hydroxyapatite, 211), 45.67 ° (hydroxyapatite, 203) and 56.52 ° (hydroxyapatite, 500) for HA crystals on 10 wt% HEC sponges. These results prove the existence of the HA crystals on the HEC sponges after 48 hours crystallization process by using SBF solution (Abdallah 2011) (Mirta 2012). The further confirmation of the presence of HA crystals was done by using FESEM-EDX. It can be seen that there are more peaks and the intensity of the peaks are increased when the concentration of the HEC sponges increased. This may be because of the HA crystals formed are more when the HEC concentration increased.

**IV. CONCLUSION**

Highly porous and stable, HEC sponges with different concentrations, 1 wt%, 3 wt%, 5 wt%, 7 wt% and 10 wt% were prepared in a green chemistry approach. The HEC sponges were successfully coated with hydroxyapatite (HA) crystals using the 20x SBF solution and characterized. The optical and SEM images showed that there is no change of the morphology of the pores after the cross-linking process. From the FTIR results obtained, the presence of acetal group at the wavenumbers around 1022.20-1025.83 cm<sup>-1</sup> had showed the cross-linking process was succeeded. FTIR results after the crystallization showed peak of PO<sub>4</sub><sup>3-</sup> and CO<sub>3</sub><sup>2-</sup> which indicate



the presence of HA crystals. This result was confirmed by using XRD and FESEM-EDX. The element composition of HA crystals was revealed, which consisted of C, O, P and Ca. The morphology and the size of the HA crystals was determined by using FESEM. From the results obtained, it showed that HA crystals synthesized were in round shape, and the size of the HA crystals increased when the concentration of the HEC sponges increased. This is due to the polar hydroxyl side groups of the HEC molecules tend to interact with  $\text{Ca}^{2+}$  during the HA crystallization process. This highly porous and stable HEC sponges coated with hydroxyapatite crystals are a promising biomaterial for bone tissue engineering.

### ACKNOWLEDGEMENT

The authors acknowledge the support from the College of Arts and sciences, University of Nizwa and TRC, sultanate of Oman.

### REFERENCES

- [1]. Abdallah A.Shaltout, Moussa A.Allam and Mohamed A.Moharram, 2011, FTIR spectroscopic, thermal and XRD characterization of hydroxyapatite from new natural sources, *Spectrochimica Acta Part A: Molecular and Biomolecular Spectroscopy*, 83- 1, 56-60.
- [2]. Azzaoui, K., Mejdoubi, E., Lamhamdi, A., Zaoui, S., Berrabah, M., Elidrissi, A., Hammouti, B., Fouda, M.M.G. and Al-Deyab, S.S. 2015. Structure and properties of hydroxyapatite/hydroxyethyl cellulose acetate composite films. *Carbohydrate Polymers*. 115: 170-176.
- [3]. Cengiz, B., Gokce, Y., Yildiz, N., Aktas, Z. and Calimli, A. 2008. Synthesis and characterization of hydroxyapatite nanoparticles. *Colloids and Surfaces A: Physicochemical and Engineering Aspects*. 322(1): 29-33.
- [4]. Chalal, S., Fathima, S.J. and Yusoff, M.B. 2014. Biomimetic growth of bone-like apatite via simulated body fluid on hydroxyethyl cellulose/polyvinyl alcohol electrospun nanofibers. *Bio-medical materials and engineering*. 24(1537): 799-806.
- [5]. Chavan, P.N., Bahir, M.M., Mene, R.U., Mahabole, M.P. and Khairnar, R.S. 2010. Study of nanobiomaterial hydroxyapatite in simulated body fluid: Formation and growth of apatite. *Materials Science and Engineering: B*. 168(1): 224-230.
- [6]. Chen, Z., Fu, Y., Cai, Y. and Yao, J. 2012. Effect of amino acids on the crystal growth of hydroxyapatite. *Materials Letters*. 68: 361-363.
- [7]. Choong, C., Triffitt, J.T. and Cui, Z.F. 2004. Polycaprolactone scaffolds for bone tissue engineering: Effects of a Calcium Phosphate Coating Layer on Osteogenic Cells. *Food and Bioproducts Processing*. 82(2): 117-125.
- [8]. Hollinger, J.O. 2012. *An introduction to biomaterials*. 2<sup>nd</sup> ed. New York: CRC Press.
- [9]. Ikeda, T., Ikeda, K., Yamamoto, K., Ishizaki, H., Yoshizawa, Y., Yanagiguchi, K., Yamada S. and Hayashi, Y. 2014. Fabrication and characteristics of chitosan sponge as a tissue engineering scaffold. *BioMed Research International*. 2014.
- [10]. Khairy M.Tohamy, MostafaMabrouk, Islam E.Soliman, Hanan H.Beherei and Mohamed, A.Aboelnasr, 2018, Novel alginate/hydroxyethyl cellulose/hydroxyapatite composite scaffold for bone regeneration: In vitro cell viability and proliferation of human mesenchymal stem cells. *International Journal of Biological Macromolecules*, 112, 448-460.
- [11]. Kokubo, T. and Takadama, H. 2006. How useful is SBF in predicting in vivo bone bioactivity?. *Biomaterials*. 27(15): 2907-2915.
- [12]. Li, J., Zhu, D., Yin, J., Liu, Y., Yao, F., and Yao, K. 2010. Formation of nano-hydroxyapatite crystal in situ in chitosan–pectin polyelectrolyte complex network. *Materials Science and Engineering: C*. 30(6): 795-803.
- [13]. Matassi, F., Nistri, L., Paez, D.C. and Innocenti, M. 2011. New biomaterials for bone regeneration. *Clinical Cases in Mineral and Bone Metabolism*. 8(1): 21-24.
- [14]. Mirta Mir, Fabi Lima Leite, Paul, Sérgio de Paula Herrmann Junior, Fabi Luiz Pissetti, Alexandre Malta Rossi, Elizabeth Lima Moreira, Yvonne Primeran Mascarenhas, 2012, XRD, AFM, IR and TGA study of nanostructured hydroxyapatite, *Mat. Res.* 15 (4), 622-627.
- [15]. O'Brien, F.J. 2011. Biomaterials & scaffolds for tissue engineering. *Materials Today*. 14(3): 88-95.
- [16]. Philips, G.O. and Nather, A. 2001. *The scientific basic of tissue transplantation*. Singapore: World Scientific Publishing Company.
- [17]. Sinha, A., Gupta, A.K., Pramanick, A.K., Nayar, S., Gunjan, M.K., Mishra, T., Bhatt, N.C., Vishwanath, N. and Das, S. 2009. Mimicking biomineralization under microgravity. *Materials Science and Engineering: C*. 29(3): 779-784.
- [18]. Tas, A.C. and Bhaduri, S.B. 2004. Rapid coating of Ti6Al4V at room temperature with a calcium phosphate solution similar to 10× simulated body fluid. *Journal of Materials Research*. 19(09): 2742-2749.
- [19]. Zhang, F., Yang, X. and Tian, F. 2009. Calcium carbonate growth in the presence of water soluble cellulose ethers. *Materials Science and Engineering: C*. 29(8): 2530-2538.
- [20]. Zhang, J., Zhan, X., Wen, X., Song, B., Ma, L. and Peng, W. 2009. Effects of ultrasonic and dispersants on shape and composition of hydroxyapatite by reflux method. *Inorganic Materials*. 45(12): 1362-1365.
- [21]. Zhou, H. and Lee, J. 2011. Nanoscale hydroxyapatite particles for bone tissue engineering. *Acta Biomaterialia*. 7(7): 2769-2781.
- [22]. Zulkifli, F.H., Shahitha, F., Yusuff, M.M., Hamidon, N.N. and Chahal, S. 2013. Cross-linking effect on electrospun hydroxyethyl cellulose/poly (vinyl alcohol) nanofibrous scaffolds. *Procedia Engineering*. 53: 689-695.